Electron capture and ionization of 33-TeV Pb ions in gas targets

H. F. Krause,[1] C. R. Vane,[1] S. Datz,[1] P. Grafström,[2] H. Knudsen,[3] U. Mikkelsen,[3] C. Scheidenberger,[4] R. H. Schuch,[5] and Z. Vilakazi[6]

[1]*Physics Division, Oak Ridge National Laboratory, P.O. Box 2008, Oak Ridge, Tennessee 37831-6377*

[2]*CERN SPS/SL Division, CH-1211 Geneva 23, Switzerland*

[3]*Institute of Physics, Aarhus University, DK-8000 Aarhus C, Denmark*

[4]*Gesellschaft für Schwerionenforschung mbh, Planckstrasse 1, D-64291 Darmstadt, Germany*

[5]*Atomic Physics Department, Stockholm University, Frescativägen 24, S-104 05 Stockholm 50, Sweden*

[6]*University of Witwatersrand, Department of Physics, 1 Jan Smuts Avenue, P.O. Wits, Johannesburg 2050, South Africa*

(Received 27 January 2000; published 13 February 2001)

We have measured the total cross sections for electron capture by bare Pb^{82+} ions and for the ionization of hydrogenlike $Pb^{81+}(1s)$ ions at 158 GeV/A, $\gamma=168$, in Ar, Kr, and Xe gas targets. At this energy, the total capture cross sections are dominated by electron capture from pair production. The capture measurements are compared with the results of several theoretical calculations and with similar measurements made with solid targets. The $Pb^{81+}(1s)$ ionization cross sections obtained, which are substantially lower than those measured in solids, agree well with recent calculations that predict saturation at high energies from target screening effects.

DOI: 10.1103/PhysRevA.63.032711 PACS number(s): 34.50.Fa, 34.80.Lx, 34.90.+q

Interactions involving heavy ions in the ultrarelativistic regime (>10 GeV/amu), where the relevant physics is best described in terms of the Lorentz factor γ, are currently a frontier in high-energy atomic collision physics [1]. Theoretical descriptions of electron-capture and ionization processes have been challenging in this regime because interactions of high-Z projectile and target species (where $Z\alpha \geqslant 0.5$) are strong enough at small impact parameters and large γ to potentially invalidate perturbation treatments. Numerous theoretical methods for treating these processes using quantum electrodynamics in the ultrarelativistic regime now exist [1–11].

An ultrarelativistic ion can capture an electron via three mechanisms: (i) radiative electron capture (REC), (ii) nonradiative capture (NRC), and (iii) electron capture from e^+e^- pair production (ECPP), in which the e^+e^- pair is produced by the intense electromagnetic pulse that arises when the projectile ion passes near a target nucleus. At high energies, capture cross sections, σ_{REC}, σ_{NRC}, and σ_{ECPP}, scale roughly as $\sim Z_T/\gamma$, $\sim {Z_T}^5/\gamma$, and $\sim {Z_T}^2 \ln \gamma$, respectively, where Z_T is the target atomic number [2]. Each process is expected to exhibit approximately the same dependence on the projectile atomic number, i.e., ${Z_p}^5$. Also, each capture process is predicted to have about the same fractional contribution in excited n states of the projectile ($\sim n^{-3}$, where n is the principal quantum number). The REC and NRC mechanisms, which dominate below the ultrarelativistic regime [12,13], become insignificant compared to ECPP for heavy targets when $\gamma > 100$. Cross sections for ionization are several orders of magnitude larger than those for capture, and thus limit the yield of one-electron ions obtainable in capture channels. The measurements reported here test theoretical predictions for capture and loss cross sections by heavy ions at the highest energy reported to date [2–11].

Previously, we reported important direct electron capture and loss measurements for very heavy ions in the ultrarelativistic regime ($\gamma=168$), where the σ_{ECPP} mechanism dominates the capture cross sections [14]. In those measurements, performed using 33-TeV Pb ions and a variety of thin solid targets, it was shown that ions formed in excited states should be increasingly ionized inside targets as the target Z_T increases. Now we report capture and ionization cross sections measured for 33-TeV Pb^{82+} ions in gas targets, where essentially all excited *nl* states formed either directly in the capture processes or in secondary collisional excitation rapidly decay to the 1*s* state between collisions. The ground-state $Pb^{81+}(1s)$ ions have the highest probability for survival in the gas cell; the $n=1$ state ionization cross section being $\sim$1/4 of that for the $n=2$ state. Under our conditions, measured capture cross sections are expected to exceed those obtained in solids; the effective capture cross section summed over ground and excited states should be $\sim 1.3\,\sigma_c(1s)$ for any Z_T [9]. In addition, it is expected that the effective electron-loss rates measured will yield the ionization cross sections for the ground state, $\sigma_1(1s)$.

The development of new relativistic ion colliders such as the Relativistic Heavy-Ion Collider (RHIC) at Brookhaven National Laboratory or the Large Hadron Collider (LHC) at CERN [2,8,15,16] has spurred interest in obtaining accurate electron capture and loss cross sections at high enough γ so that beam lifetimes can be accurately predicted. The cross section for the ECPP process is of practical interest to collider designers because the lower charge-state projectiles produced are lost from the beam circulating in a ring. A significant loss rate of these ions by ECPP and also by electromagnetic nuclear loss processes limits the ion storage time. These machines will operate at an effective γ of 2.3×10^4 and 1.7×10^7, respectively. For γ above $\sim$100, $\sigma_{\mathrm{ECPP}}=A\ln(\gamma)+B$, where A and B are independent of γ to within higher orders of $1/\gamma$ [4]. Total electron capture and loss measurements were reported by Claytor *et al.* [12] for $\gamma=12.6$-Au ions, but the ECPP mechanism is not prominent at this low γ, and simple $\ln(\gamma)$ scaling is not expected to be valid.

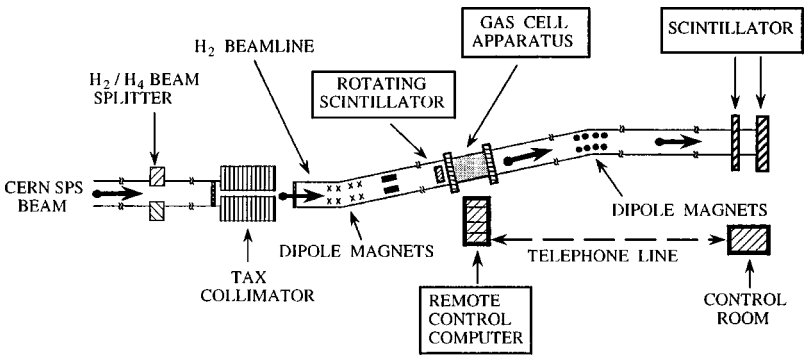

FIG. 1. Simplified diagram of the experimental setup.

Total capture and ionization cross sections were measured using the 33-TeV Pb beam at the CERN Super Proton Synchrotron (SPS). The experimental arrangement is shown schematically in Fig. 1. The Pb^{82+} beam exiting the SPS traversed about 5 m of air and passed through a thin vacuum window (100-μm Al) as it entered the evacuated beamline. In one set of measurements called the ''capture experiment,'' collimated $^{208}Pb^{82+}$ ions were mass and charge-state selected at the first magnetic bend and traveled ~300 m in vacuum (~10 mTorr) before impinging on a 2.4-m-long gas cell with thin Mylar windows. A second magnetic bend and collimator, located ~100 m beyond the gas cell, were set to transmit all $^{208}Pb^{81+}$ ions leaving the cell. The ion intensity at the end of the 800-m-long beamline was measured as a function of gas pressure using coincidence signals from fast scintillators. The same setup was used in a second set of measurements called the ''ionization experiment,'' except that the full beamline was tuned to transmit $^{208}Pb^{81+}$ ions, so that surviving one-electron ions were measured. The incident $Pb^{81+}(1s)$ ions were formed by electron capture prior to entering the evacuated line [$\sim 1.65\times 10^{-3}\times(Pb^{82+}$ intensity)]. At 10-m Torr pressure, the background gas thickness in the beamline was low enough to limit collisional loss of the Pb^{81+} ions to less than ~1% before magnetic analysis and detection.

The gas cell consisted of modified high-vacuum pneumatic valves (with 50-μm-thick mylar entrance and exit windows) separated by beam pipe (with an effective length of 2.352 m). The pressure of target gases introduced into the cell (maximum pressures of 300, 80, and 70 Torr for Ar, Kr, and Xe, respectively) was controlled by a gas manifold with a vacuum pump using an array of solenoid valves; the valves and cell windows were remotely controlled by a Macintosh computer located at the cell. Pressure in the cell, monitored on two capacitance manometer gauges (Baratron 100- and 1000-μm full scale), was measured absolutely to within $\pm 0.1\%$ of full scale. The gas density in the cell could be calculated from the pressure readings without loss of precision by knowing the cell temperature, which was measured by two calibrated thermistors (± 0.1 °C) that were mounted in thermal contact with the cell. The 1000-μm gauge was calibrated absolutely against a precision barometer at air pressure before the experiments were performed ($\pm 0.01\%$).

The Pb^{82+} ion beam came in 5-sec spills ($\sim 10^5$ ions/spill) every 20 sec from the CERN SPS. The Pb^{82+} beam intensity was measured on a CERN beam monitor located ahead of our beamline. The Pb^{82+} beam at the target gas cell was also monitored during the capture experiments using a rotating thin plastic scintillator that sampled the beam (duty factor ~7.6%) [17]. Data acquisition and control for the rotating scintillator and gas cell located in the CERN beam tunnel were controlled remotely by telephone connection between two Macintosh computers.

Experimental data illustrating the growth of the Pb^{81+} ion fraction vs Xe target thickness (''capture experiment'') are shown in Fig. 2(a). Data illustrating the loss of the Pb^{81+} ion fraction vs Xe target thickness (''ionization experiment'') are shown in Fig. 2(b). These raw data, corrected for an experimentally determined 9.5% ionization loss in each thin mylar window, were used to determine the effective cross sections for capture (σ_c) and loss (σ_i) processes. Because σ_c is orders of magnitude smaller than σ_i, only two charge states (Pb^{81+} and Pb^{82+}) need to be considered and solutions to the coupled differential equations describing charge-state evolution as a function of gas target thickness reduce to simple analytical forms. The cross sections were determined for capture by Pb^{82+} and the ionization of Pb^{81+} by fitting data obtained in the ''capture experiment'' [Fig. 2(a)] using

$$F(81)=F_{\mathrm{eq}}\{1-\exp[-(\sigma_c+\sigma_i)t]\}\exp[-\sigma_n t], \qquad (1)$$

where $F(81)$ is the fraction of surviving Pb^{81+} ions, σ_c is the total capture cross section, σ_i is the total ionization cross section, σ_n is the total cross section for beam loss by nuclear reactions (all in cm^2), t is the target thickness (atoms/cm^2), and $F_{\mathrm{eq}}=[\sigma_c/(\sigma_c+\sigma_i)]$ is the equilibrium Pb^{81+} charge-state fraction. The σ_n used for Ar, Kr, and Xe are 9.2, 19.9, and 34.4 b, respectively; these are interpolated values based on fits to measurements made previously for a variety of elemental solid targets [18]. In the ''ionization experiment'' [Fig. 2(b)], the surviving fraction of Pb^{81+} ions is given by

$$F(81)=\{[1-F_{\mathrm{eq}}]\exp[-(\sigma_c+\sigma_i)t]+F_{\mathrm{eq}}\}\exp[-\sigma_n t]. \qquad (2)$$

Here, the slope of the exponential fit to the survival charge fraction yields $\sigma_i+\sigma_c$ directly. The nuclear loss term in Eqs. (1) and (2) was found to be an insignificant correction for each gas.

Electron-capture cross sections obtained from fits to data in the ''capture experiment'' using this two-state model have contributions from one-electron ions formed in all possible

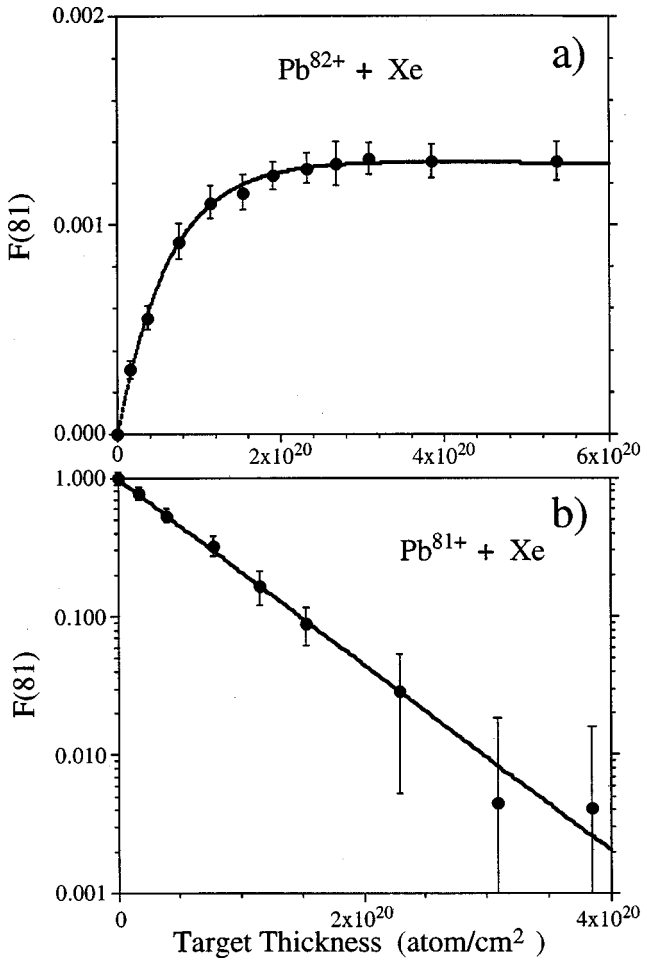

FIG. 2. (a) Fraction of one-electron Pb^{81+} ions vs Xe target thickness measured in the ''capture experiment.'' The solid curve is the growth curve [Eq. (1)] calculated using the cross sections σ_c and σ_i obtained via a least-squares fitting procedure. (b) Logarithmic plot of the surviving fraction of $Pb^{81+}(1s)$ ions versus Xe target thickness measured in the ''ionization experiment.'' The experimental equilibrium fraction was subtracted from each value before fitting, thus the slope yields σ_i essentially. The least-squares fit to the data is shown.

final states. Calculations for photon impact pair production with capture using relativistic Coulomb scattering states [9] predict that excited ion states will contribute ~30% to the total cross sections of σ_{ECPP}, when additional contributions from $2p$ and higher states are included ($\sim n^{-3}$ distribution). Excited *ns* metastable states are favored over the much shorter lived *np* excited states (e.g., for $2s$, the predicted fraction is ~70% of the overall excited-state contribution). Similar predictions have been made by Baltz [8]. The $2s$ state, populated directly or from cascade contributions from higher *nl* states, decays in the projectile frame with the rate $A(2s)=5.521\times10^{13}$/s (sum for the magnetic dipole, $M1$, and simultaneous two-photon electric dipole, $2E1$, decay modes) [19–20]. Correcting for time dilatation in the laboratory frame, this slow $2s$ decay rate translates to a decay length of ~1 mm in the laboratory frame {inverse decay length$=A(2s)/[\gamma c]$ of 10.95 /cm}. The $2s$-state decay rate is the rate limiting step for all excited-state decay, because

TABLE I. Measured cross sections for electron capture and ionization by 33-TeV Pb ions in gas targets.

		Capture		Ionization σ_{ioniz} (kb)	
Target	Z_T	$\sigma_{\mathrm{Cap}}(b)$	$\sigma_{\mathrm{ECPP}}(b)$	Cap. expt.	Ioniz. expt.
Ar	18	2.9	2.5±0.2	1.88±0.13	1.97±0.14
Kr	36	10.1	9.4±0.7	6.80±0.48	7.38±0.52
Xe	54	20.7	19.4±1.4	15.5±1.1	15.7±1.1

dipole-allowed transition rates for $Pb^{81+}(2p\rightarrow1s)$ and for decay from higher excited states are much faster than the $2s\rightarrow1s$ transition rate [e.g., $A(2p\rightarrow1s)=2.245\times10^{16}$/s] [21]. More than 99% of the $2s$ population formed in capture decays to the $1s$ state without being ionized in secondary collisions for most of our gas target conditions because the $2s$ decay rate is orders of magnitude faster than the collisional ionization loss rate. In the worst case, Xe, at the highest gas pressure, using [assuming $\sigma_i(Z_T)\sim {Z_T}^2$, and $\sigma_i{}^*\sim n^2\sigma_i(1s)$] the $2s$ radiative decay to $1s$, is still 98.6% [$N\sigma_i=0.14$/cm, where $n=2$ and $N=2.28\times10^{18}$/cm^3 at a cell pressure of 70 Torr]. Therefore the two-state approximation discussed above and used to analyze gas data gives the capture cross section summed over all final states and the $1s$ ionization cross section, independent of the actual *nl* distributions formed in the capture process. We have also verified this conclusion by adding collisional excitation process channels in model calculations that track excited-state populations in solutions of *n*-state fully coupled differential equations.

The experimental capture and ionization cross sections for each target species are listed in Table I. The overall uncertainty of about ±7% includes fitting (statistical) errors and estimated systematic uncertainties. Each measured total capture cross section (σ_c) is the sum of three processes, $\sigma_c=\sigma_{\mathrm{ECPP}}+\sigma_{\mathrm{REC}}+\sigma_{\mathrm{NRC}}$. Subtracting calculated values [2] of σ_{NRC} (which amount to less than 2%) and fitted values of σ_{REC} from the total capture cross section for each target gas yields the σ_{ECPP} values listed in Table I. The fitted REC cross sections were derived from an analysis of experimental data for measured total capture cross sections in Be, C, Al, Cu, Sr, and Au [22]. These experimental REC cross sections are ~20% larger than the calculated REC cross sections [2], but the difference has little effect on the σ_{ECPP}, especially for heavy gases.

Three theoretical values for σ_{ECPP} are available. The perturbative estimate of Anholt and Becker [2] (with screening) is given in tables for each projectile and target. The nonperturbative calculation of Bottcher and Strayer [3], obtained specifically for capture to $1s$ at $\gamma=168$ for the Pb-Au system, by solving the time-dependent Dirac equation, yielded $\sigma_{\mathrm{ECPP}}(1s)=50$ b. The nonperturbative calculations of Baltz *et al.* [8] yielded $\sigma_{\mathrm{ECPP}}(1s)=46$ b. In comparisons to be discussed, the σ_{ECPP} have been scaled to each target gas according to $[{Z_T}^2+Z_T]$, as recommended by Anholt and Becker (${Z_T}^2$ dependence with an ''antiscreening'' correction for Z_T independent electrons).

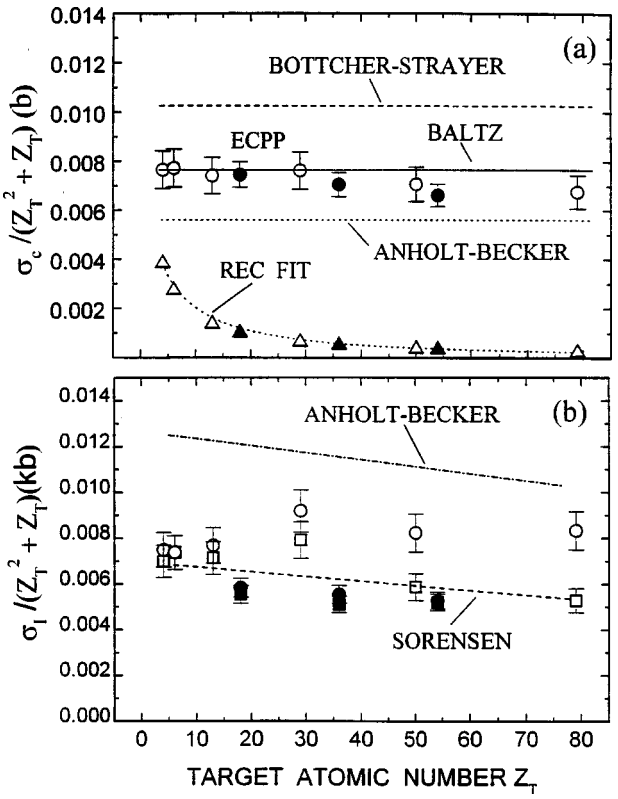

FIG. 3. Measured cross sections for 158 GeV/A, $\gamma=168$, Pb^{82+}, and Pb^{81+} electron capture and ionization: (a) electron-capture cross sections for gas targets (●) and solid targets (○) compared with calculations for ECPP. REC fit data (▲, △) indicate contributions from REC that have been subtracted from the total capture to obtain the ECPP values. (b) Measured ionization cross sections compared with theory. [(●, ○) and (■, □) indicate measurements from the ''capture experiment'' and the ''ionization experiment,'' respectively.]

Comparisons of experimental and theoretical σ_{ECPP} are presented as functions of Z_T in Fig. 3(a) with all cross sections normalized to $(Z_T{}^2+Z_T)$. We note exceptionally good agreement between experiment and $1s$ calculations by Baltz *et al.* and Anholt and Becker. We note that the measured σ_{ECPP} are nearly equal to the calculated cross sections for capture to the $Pb^{81+}(1s)$ ground state alone, i.e., ~30% lower than predictions for capture to all final states. We also note that the electron-capture cross sections in the gas targets are approximately the same as would be interpolated from our previously measured results in solid-elemental targets [14]. This equivalence is unexpected because capture from gas targets should include an extra contribution from excited-state captured electrons, some of which would be ionized in solid targets—especially for high Z_T.

In Fig. 3(b), we compare the ionization cross sections obtained from both the growth (''capture experiment'') and decay (''ionization experiment'') curves, given in Table I, to the most recent ''ion-atom'' theoretical values of Sørensen for $Pb^{81+}(1s)$ [11]. Both experimental and theoretical values are normalized to $(Z_T{}^2+Z_T)$. The cross sections obtained by the two methods for each target are expected to agree in gases, despite possible differing degrees of product excitation, because excited states decay to $1s$ before ionization can occur. The older predictions of Anholt and Becker, which are about a factor of 2 larger than our measurements, are also shown. Sørensen [11] has pointed out that when $\gamma \gg 5$, the maximum effective impact parameter for the γ-dependent term of σ_i used by Anholt and Becker, is limited by atomic target electron screening. When the maximum adiabatic distance for producing ionization via the time-dependent pulse in the collision (used by Anholt and Becker) exceeds the smaller Thomas-Fermi screening radius, then the latter must be used as an upper impact-parameter cutoff. This correction due to screening leads to ''saturation'' of the ionization cross section for $\gamma \gg 5$. Sørensen also suggested other ways for improving the theoretical σ_i estimates beyond the approximations he has used. These improvements have not yet been implemented in the calculations.

The excellent agreement of ionization cross sections obtained in our two independent experiments (e.g., ''capture'' vs ''ionization'' gas target experiments) also suggests that the capture cross sections are not seriously flawed. The ionization cross sections would not agree, for example, if the transmission functions for Pb^{81+} and Pb^{82+} beams were different; the Pb^{82+} transmission is needed to derive the equilibrium fraction, σ_c and σ_i from capture experiments, but the Pb^{82+} transmission is not needed in the ionization experiment.

Comparing gas and solid results in the ''ionization'' experiment for targets of comparable Z_T, we find that the effective ionization cross sections in solid targets are about 25% larger than in gas. Direct excitation of a small fraction of the $Pb^{81+}(1s)$ beam to form dipole-allowed np final states, which can be ionized in solid targets, can explain the gas-solid difference for $Z_T=18$ and above. Competition between radiative decay and ionization rates of the excited state in solids and no competition in gas targets again explains the difference. The mean-free path for radiative decay of $Pb^{81+}(2p)$ ions formed is 2.3×10^{-4} cm in the laboratory frame. In Sn ($Z_T=50$), for example, the mean-free path for ionization of $2p$ ions is 6×10^{-4} cm [assuming that the $2p$ ionization cross section is $4\sigma_i(1s)$]. Therefore about 30% of the ions excited to the $2p$ state are ionized in the Sn target before decay to $1s$. Essentially all of the $2s$ ions formed are also ionized in Sn.

The equilibrium fractions, $F_{\mathrm{eq}}(81)=\sigma_c/(\sigma_c+\sigma_i)$, obtained in the ''capture'' analysis are 1.44×10^{-3}, 1.37×10^{-3}, and 1.32×10^{-3} for Ar, Kr, and Xe, respectively. These are slightly lower than the equilibrium value for air ($\sim1.65\times10^{-3}$) obtained by other means, which provided the input $Pb^{81+}(1s)$ beam for the ''ionization'' experiment. The inert gas equilibrium values are 20–30% larger than those in solid targets of comparable Z_T, essentially because the effective σ_i measured for gas targets are significantly lower than in solid targets.

In summary, our experiments have isolated the ECPP mechanism for capture. Following theoretical predictions, we expected the ECPP cross sections summed over all final states to be about $1.3\sigma_c(1s)$. Instead, the measured capture cross sections were found to be the same as $\sigma_c(1s)$, and the cross sections increasingly fall below theoretical expectation

as Z_T increases. The gas target-capture cross sections agree with those measured in solids indicating less capture to excited states than predicted by theory. These results suggest at least two possibilities: (i) If the theoretically predicted excited fraction is correct, then the expected theoretical scaling for capture is slower than $({Z_T}^2+Z_T)$; (ii) if the correct scaling for $\sigma_{\mathrm{ECPP}}(Z_T)$ is $\sim({Z_T}^2+Z_T)$, then the theoretically predicted excited-state fraction has been over estimated for $Z_T > 17$. The $1s$ ionization cross sections obtained in our independent gas target experiments agree well with Sørensen's recent estimates and with each other. The larger ionization cross sections observed in solids can be attributed to an additional channel of secondary ionization of collisionally excited states. The Pb^{81+} equilibrium fractions obtained in gas targets are 20–30% larger than in solid targets of comparable Z_T, because of the lower effective ionization cross sections in gases (complete relaxation of excited states formed).

The authors H.E.K., C.R.V., and S.D. acknowledge support by the U.S. DOE Office of Basic Energy Sciences, Division of Chemical Sciences, under Contract No. DE-AC05-96OR22464 with Lockheed Martin Energy Research Corporation. H.K. acknowledges the support of the Danish Natural Science Research Council.

[1] For reviews of relativistic ion-atom collisions see, for example, J. Eichler and W. E. Meyerhof, *Relativistic Atomic Collisions* (Academic Press, San Diego, 1995); R. Anholt and H. Gould, in *Advances in Atomic and Molecular Physics*, edited by D. Bates and B. Bederson (Academic Press, Orlando, 1986), pp. 315–386; references contained therein.
[2] R. Anholt and U. Becker, Phys. Rev. A **36**, 4628 (1987).
[3] C. Bottcher and M. R. Strayer, Phys. Rev. Lett. **54**, 669 (1985); Phys. Rev. D **39**, 1330 (1989); private communications.
[4] A. J. Baltz, M. J. Rhoades-Brown, and J. Weneser, Phys. Rev. A **44**, 5569 (1991); **47**, 3444 (1993); **48**, 2002 (1993); **50**, 4842 (1994).
[5] A. Aste, K. Hencken, D. Trautmann, and G. Baur, Phys. Rev. A **50**, 3980 (1994).
[6] M. C. Güclü, J. C. Wells, A. S. Umar, M. R. Strayer, and D. J. Erust, Phys. Rev. A **51**, 1836 (1995).
[7] K. Momberger, A. Belkacem, and A. H. Sørensen, Phys. Rev. A **53**, 1605 (1996).
[8] A. J. Baltz, M. J. Rhoades-Brown, and J. Weneser, Phys. Rev. E **54**, 4233 (1996).
[9] C. K. Agger and A. H. Sørensen, Phys. Rev. A **55**, 402 (1997).
[10] Calculation of ionization cross sections, A. J. Baltz (private communication).
[11] A. H. Sørensen, Phys. Rev. A **58**, 2895 (1998).
[12] N. Claytor, A. Belkacem, T. Dinneen, B. Feinberg, and Harvey Gould, Phys. Rev. A **55**, R842 (1997).
[13] See, for example, A. Ichihara, T. Shirai, and Jörg Eichler, Phys. Rev. A **49**, 1875 (1994); P. H. Mokler and Th. Stöhlker, in Adv. At., Mol., Opt. Phys. **37**, 297 (1996).
[14] H. F. Krause, C. R. Vane, S. Datz, P. Grafström, H. Knudsen, C. Scheidenberger, and R. H. Schuch, Phys. Rev. Lett. **80**, 1190 (1998).
[15] D. Brandt, K. Eggert, and A. Morsch, CERN Report No. AT/94-05, 1994 (unpublished).
[16] P. Grafström, S. Datz, H. F. Krause, C. R. Vane, H. Knudsen, U. Mikkelsen, R. H. Schuch, C. Scheidenberger, and Z. Vilakazi, CERN Report No. SL-99-033-EA, 1999 (unpublished); *1999 International Accelerator Conference Proceedings* (IEEE, Piscataway, NJ, 1999), Vol. 3, pp. 1671–1673.
[17] H. F. Krause, E. F. Deveney, N. L. Jones, C. R. Vane, S. Datz, H. Knudsen, P. Grafström, and R. H. Schuch, Nucl. Instrum. Methods Phys. Res. B **124**, 128 (1997).
[18] S. Datz, H. F. Krause, C. R. Vane, H. Knudsen, P. Grafström, and R. H. Schuch, Phys. Rev. Lett. **77**, 2925 (1996); S. Datz, J. R. Beene, P. Grafström, H. Knudsen, H. F. Krause, R. H. Schuch, and C. R. Vane, *ibid.* **79**, 3355 (1997).
[19] W. R. Johnson, Phys. Rev. Lett. **29**, 1123 (1972).
[20] G. W. F. Drake, Phys. Rev. A **34**, 2871 (1986).
[21] W. L. Wiese and G. A. Martin, in *Physics Vade Mecum*, edited by H. L. Anderson (AIP, New York, 1989), p. 99.
[22] C. R. Vane, H. F. Krause, S. Datz, P. Grafström, H. Knudsen, C. Scheidenberger, and R. H. Schuch, Phys. Rev. A. **62**, 010701(R) (2000).